Synthesis, Photophysics, and Reverse Saturable Absorption of 7-(Benzothiazol-2-yl)-9,9-di(2-ethylhexyl)-9*H*-fluoren-2-yl Tethered $[Ir(bpy)(ppy)_2]PF_6$ and $Ir(ppy)_3$ Complexes (bpy = 2,2'-Bipyridine, ppy = 2-Phenylpyridine)

Zhongjing Li,[†] Hui Li,[†] Brendan J. Gifford, Wadumesthrige D. N. Peiris, Svetlana Kilina, and Wenfang Sun[*]

Department of Chemistry and Biochemistry, North Dakota State University, Fargo, ND 58108-6050

[*]Phone: 701-231-6254; E-mail: Wenfang.Sun@ndsu.edu

[†]These two authors contribute equally to this project.

***fac*-3**

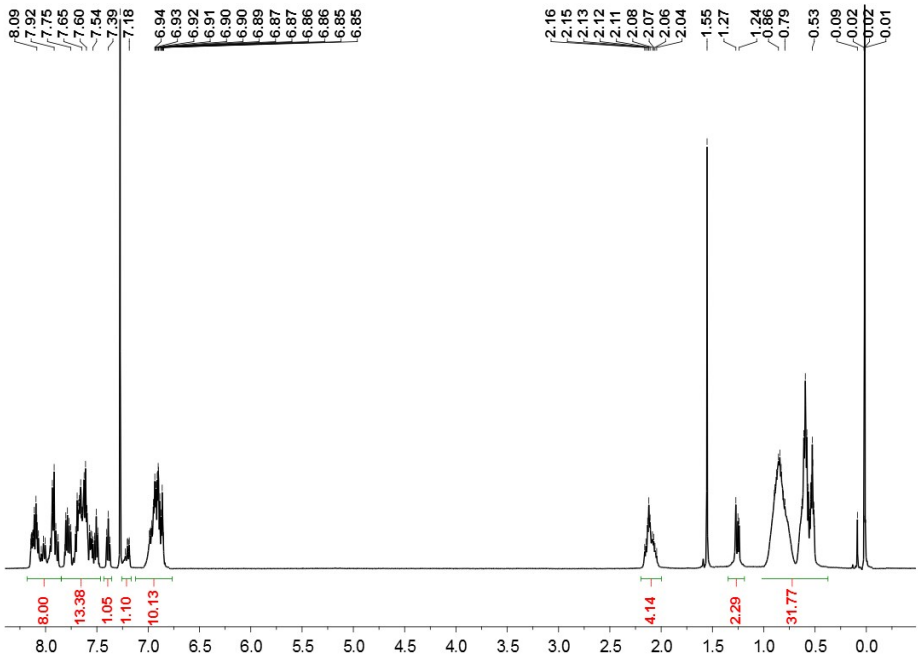
8.09
7.92
7.77
7.75
7.65
7.60
7.54
7.39
7.18
6.94
6.93
6.92
6.91
6.90
6.90
6.89
6.87
6.87
6.86
6.86
6.85
6.85
2.16
2.15
2.13
2.12
2.11
2.08
2.07
2.06
2.04
1.55
1.27
1.24
0.86
0.79
0.53
0.09
0.02
0.02
0.01
8.00
13.38
1.05
1.10
10.13
4.14
2.29
31.77
8.0 7.5 7.0 6.5 6.0 5.5 5.0 4.5 4.0 3.5 3.0 2.5 2.0 1.5 1.0 0.5 0.0

***fac*-4**

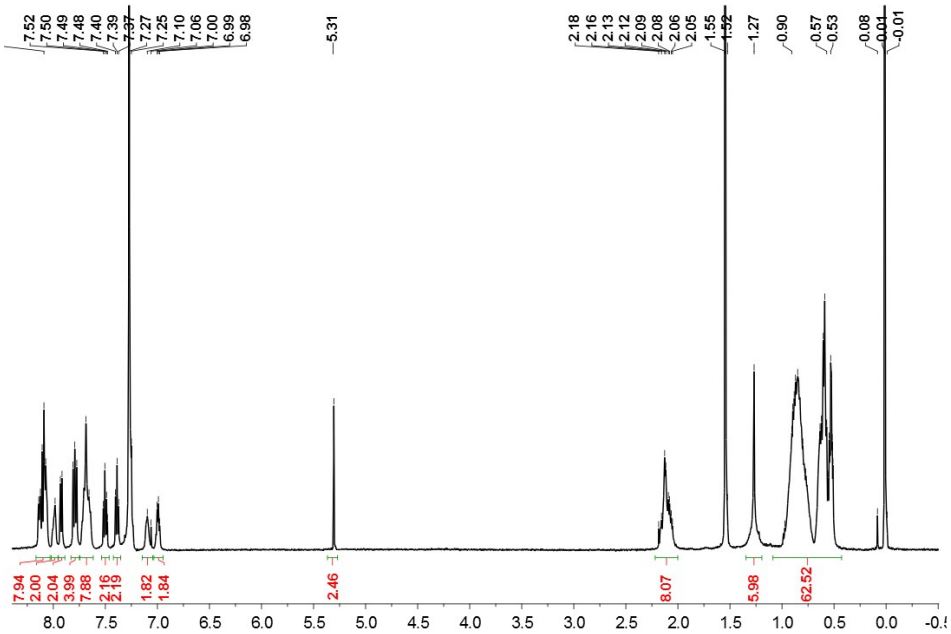
7.52
7.50
7.49
7.48
7.40
7.39
7.37
7.27
7.25
7.10
7.06
7.00
6.99
6.98
5.31
2.18
2.16
2.13
2.12
2.09
2.08
2.06
2.05
1.55
1.52
1.27
0.90
0.57
0.53
0.08
0.01
-0.01
7.94
2.00
2.04
3.99
7.88
2.16
2.19
1.82
1.84
2.46
8.07
5.98
62.52
8.0 7.5 7.0 6.5 6.0 5.5 5.0 4.5 4.0 3.5 3.0 2.5 2.0 1.5 1.0 0.5 0.0 -0.5

***fac*-5**

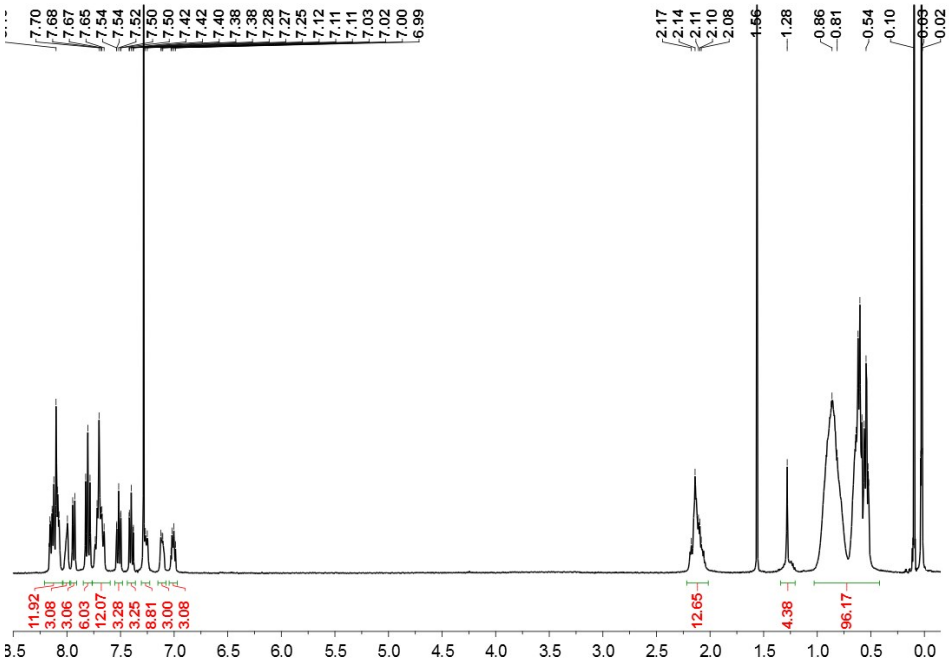
7.70
7.68
7.67
7.65
7.54
7.54
7.52
7.50
7.50
7.42
7.42
7.40
7.38
7.38
7.28
7.27
7.25
7.12
7.11
7.11
7.03
7.02
7.00
6.99
2.17
2.14
2.11
2.10
2.08
1.56
1.28
0.86
0.81
0.54
0.10
0.03
0.02
11.92
3.08
3.06
6.03
12.07
3.28
3.25
8.81
3.00
3.08
12.65
4.38
96.17
8.0
7.5
7.0
6.5
6.0
5.5
5.0
4.5
4.0
3.5
3.0
2.5
2.0
1.5
1.0
0.5
0.0

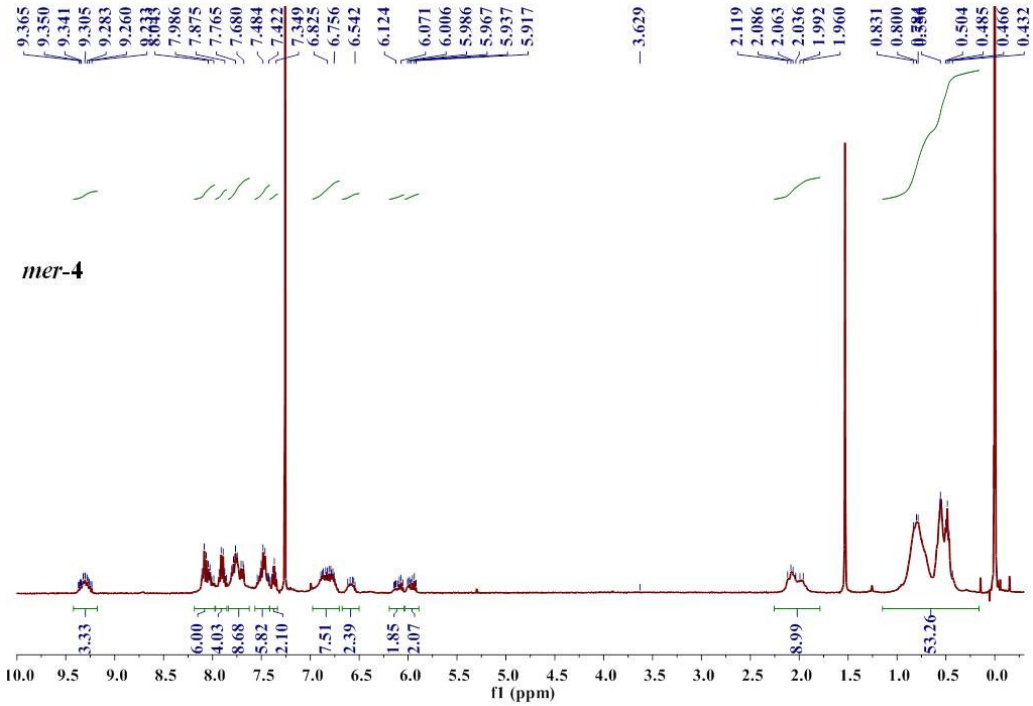
9.365
9.350
9.341
9.305
9.283
9.260
7.986
7.875
7.765
7.680
7.484
7.422
7.349
6.825
6.756
6.542
6.124
6.071
6.006
5.986
5.967
5.937
5.917
3.629
2.119
2.086
2.063
2.036
1.992
1.960
0.831
0.800
0.504
0.485
0.466
0.432
mer-4
3.33
6.00
4.03
8.68
5.82
2.10
7.51
2.39
1.85
2.07
8.99
53.26
10.0
9.5
9.0
8.5
8.0
7.5
7.0
6.5
6.0
5.5
5.0
4.5
4.0
3.5
3.0
2.5
2.0
1.5
1.0
0.5
0.0
f1 (ppm)

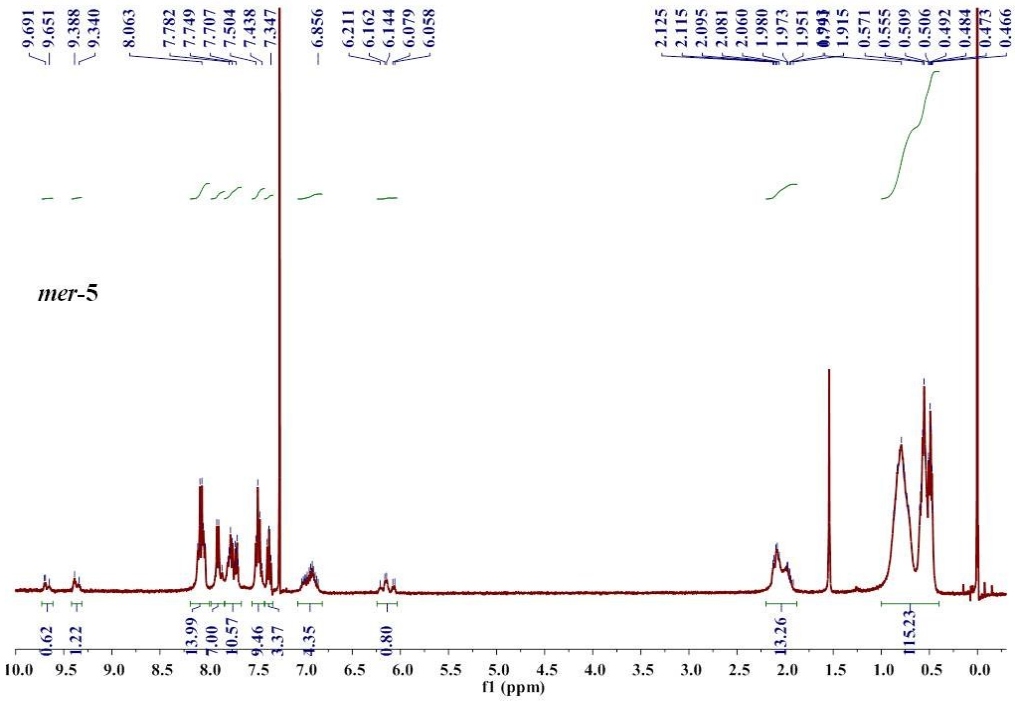

Figure S1. ^{1}H-NMR spectra of *fac*-isomers of **3 - 5** and *mer*-isomers of **4** and **5** in $CDCl_3$.

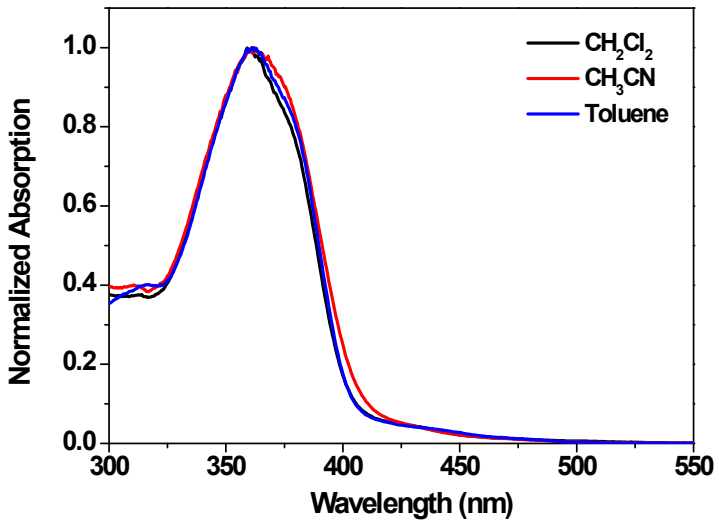

Figure S2. Normalized electronic absorption spectra of **1** in different solvents.

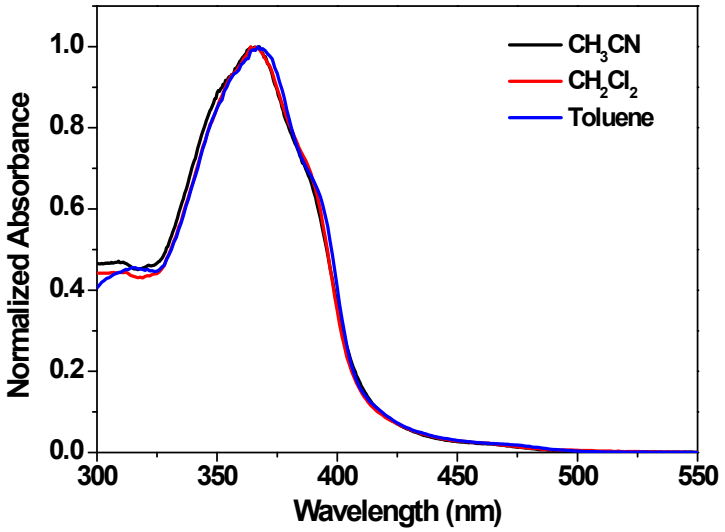

Figure S3. Normalized electronic absorption spectra of **2** in different solvents.

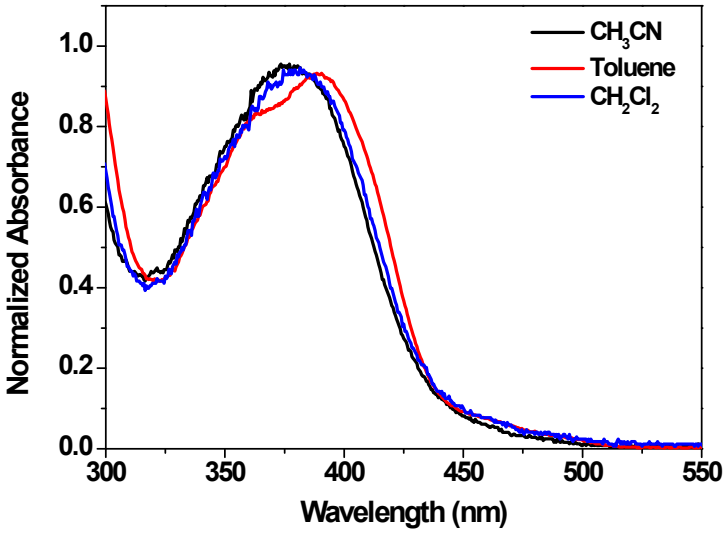

Figure S4. Normalized electronic absorption spectra of **3** in different solvents.

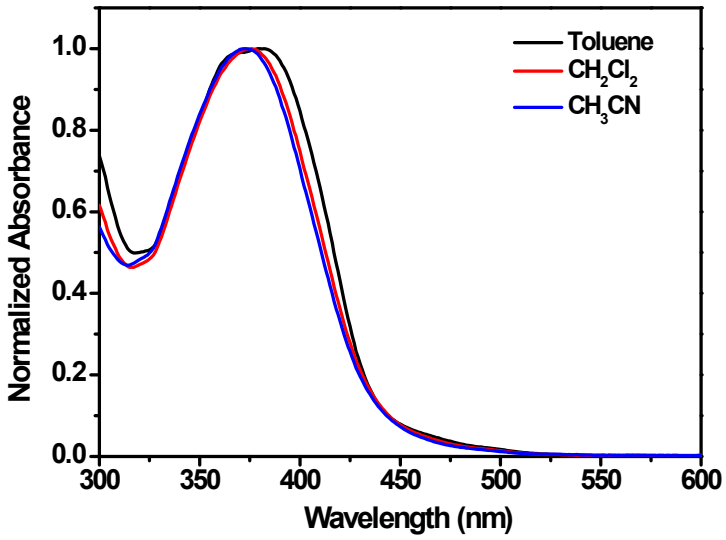

Figure S5. Normalized electronic absorption spectra of **4** in different solvents.

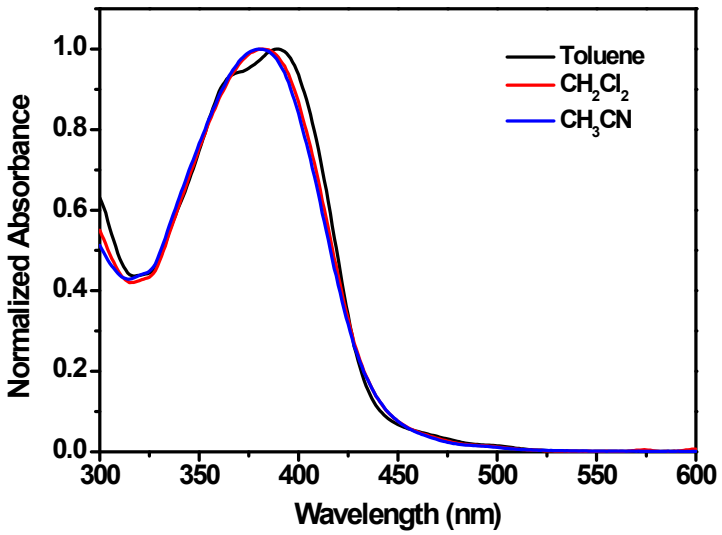

Figure S6. Normalized electronic absorption spectra of **5** in different solvents.

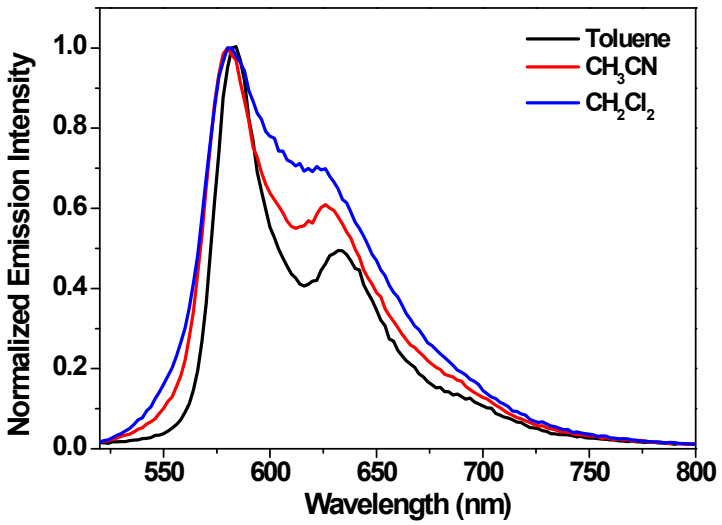

Figure S7. Normalized emission spectra of **1** in different solvents (λ_{ex} = 436 nm).

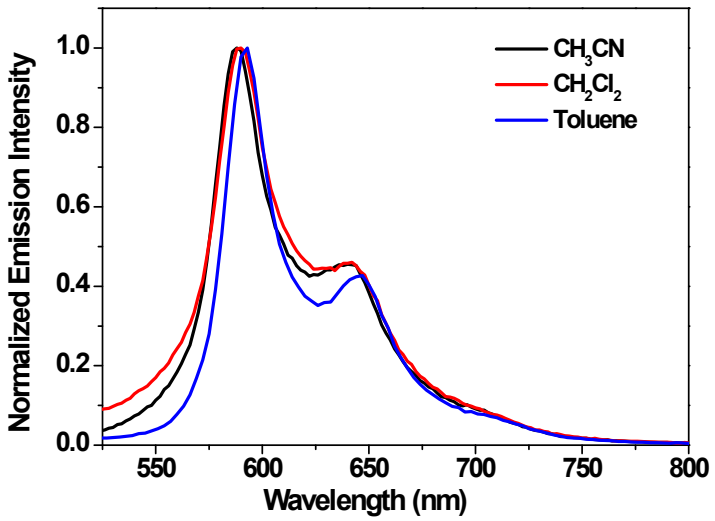

Figure S8. Normalized emission spectra of **2** in different solvents (λ_{ex} = 436 nm).

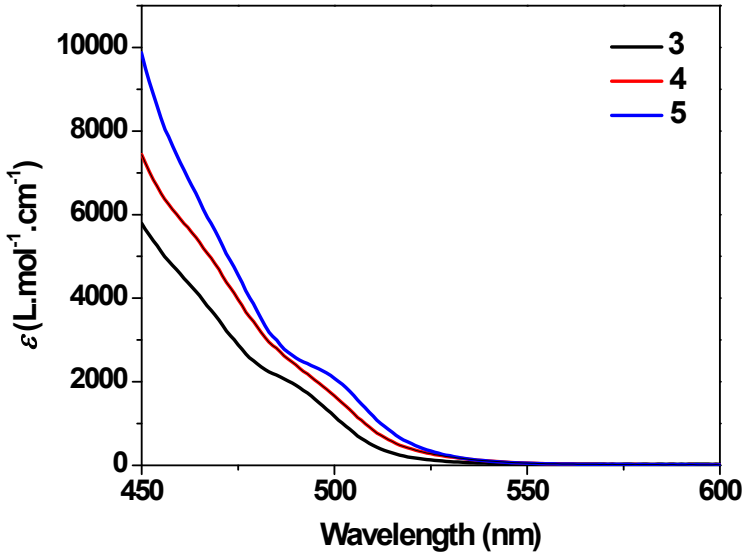

Figure S9. UV-vis absorption spectra of **3** – **5** in toluene in the region of 450-600 nm.

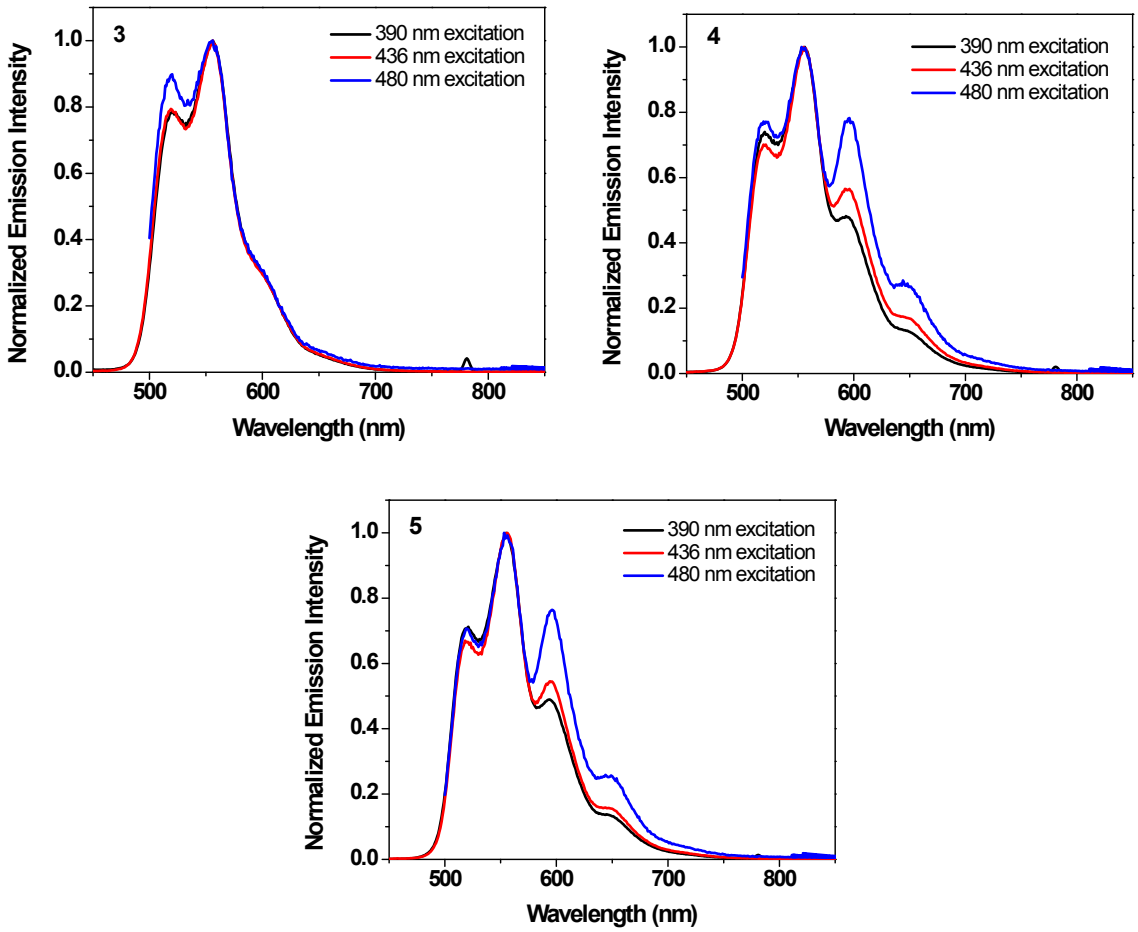

Figure S10. Normalized emission spectra of **3 - 5** in toluene at different excitation wavelengths.

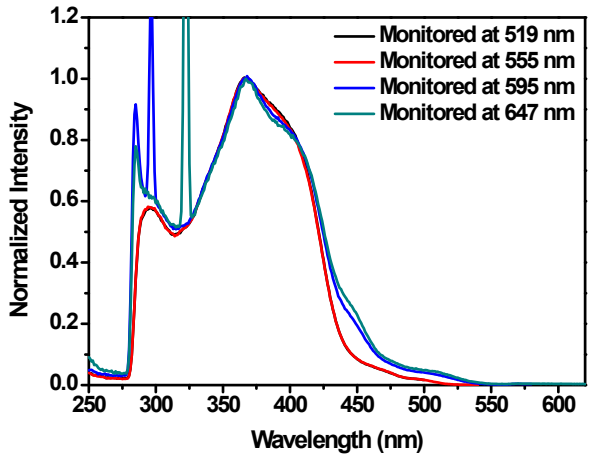

Figure S11. Normalized excitation spectra of **5** in toluene when monitored at different emission wavelengths.

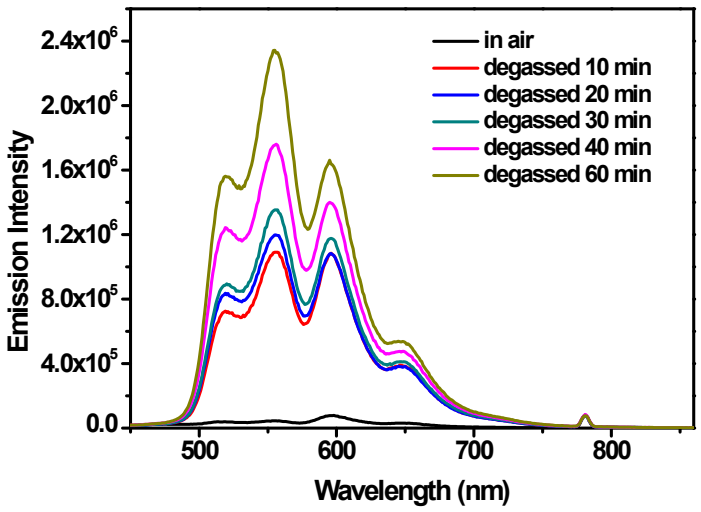

Figure S12. Emission spectra of **5** in toluene under different deaeratation conditions. λ_{ex} = 390 nm.

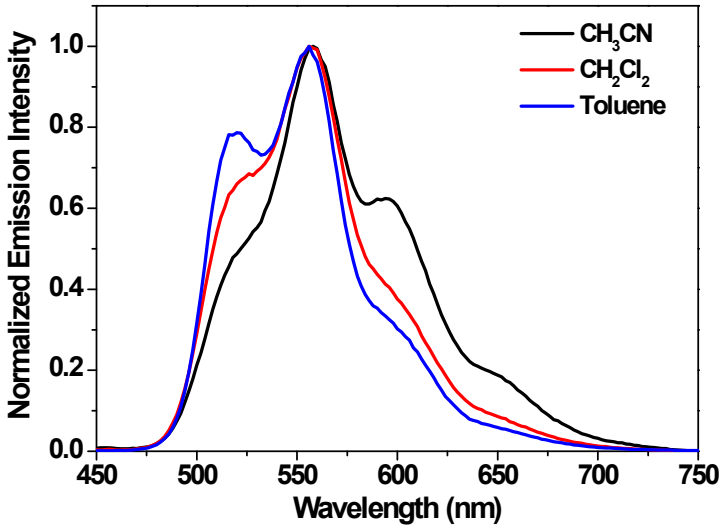

Figure S13. Normalized emission spectra of **3** in different solvents (λ_{ex} = 436 nm).

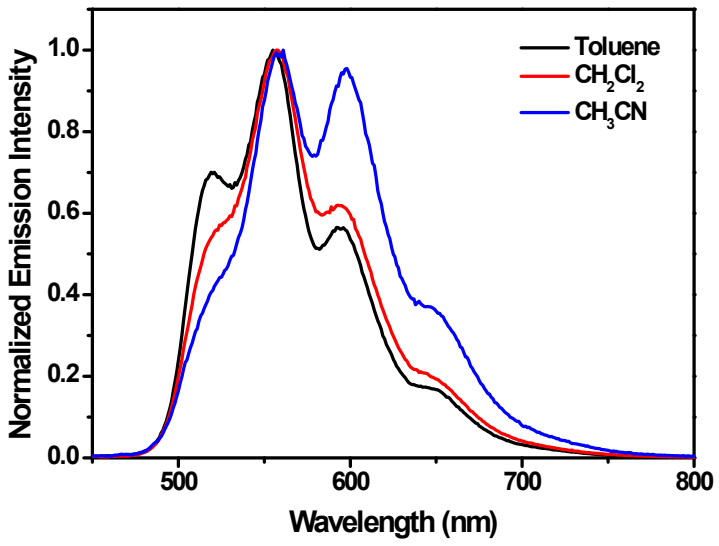

Figure S14. Normalized emission spectra of **4** in different solvents (λ_{ex} = 436 nm).

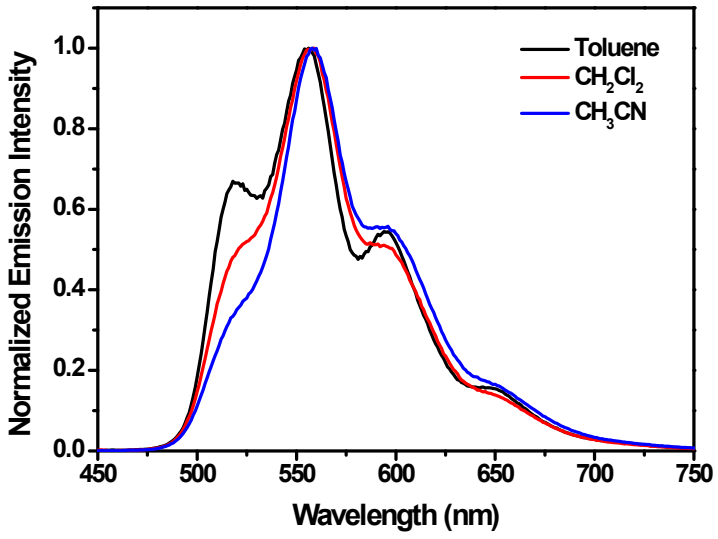

Figure S15. Normalized emission spectra of **5** in different solvents (λ_{ex} = 436 nm).

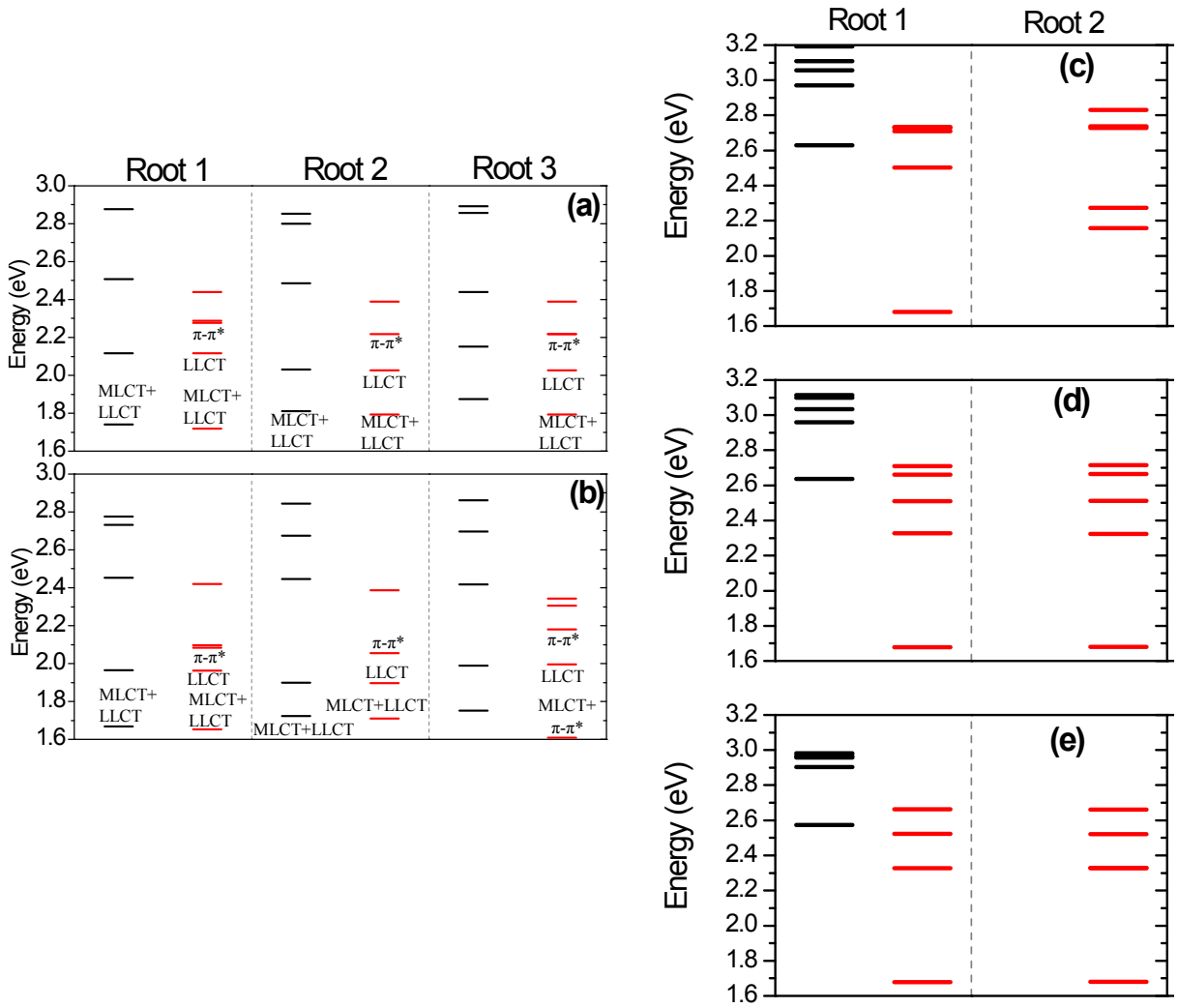

Figure S16. The calculated emission state diagram for complexes **1** (a), **2** (b), **3** (c), **4** (d), and **5** (e). Black lines indicate the singlet states, and red lines indicate the triplet states. For optimization of the lowest excited state, we started with several different initial guesses for the wavefunction choosing either the very lowest triplet state (root = 1) or the second lowest triplet state (root = 2) or the third lowest state (root = 3) initially taken at the ground state geometry of the triplet state. Similar approaches have been used for optimization of the singlet states using each of the three lowest singlet states at their ground state geometry. By starting with different initial wavefunctions, we were able to converge to different triplet or singlet states. The predominating character of the electronic states is also defined.

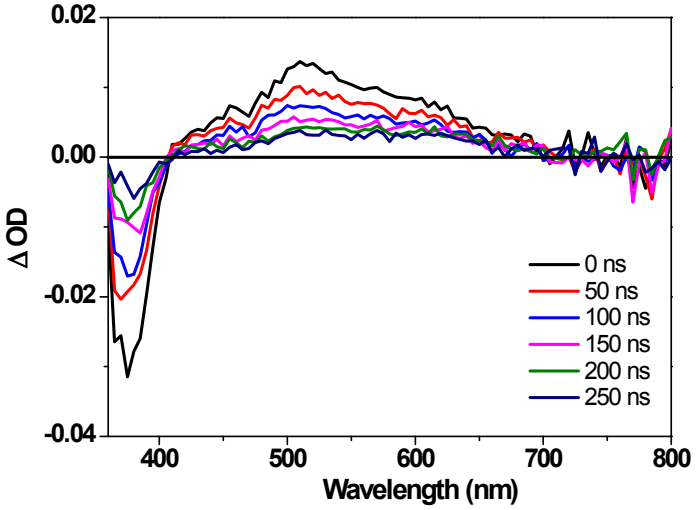

Figure S17. Time-resolved transient difference absorption spectra of **1** in toluene (λ_{ex} = 355 nm, A_{355} = 0.4 in a 1-cm cuvette).

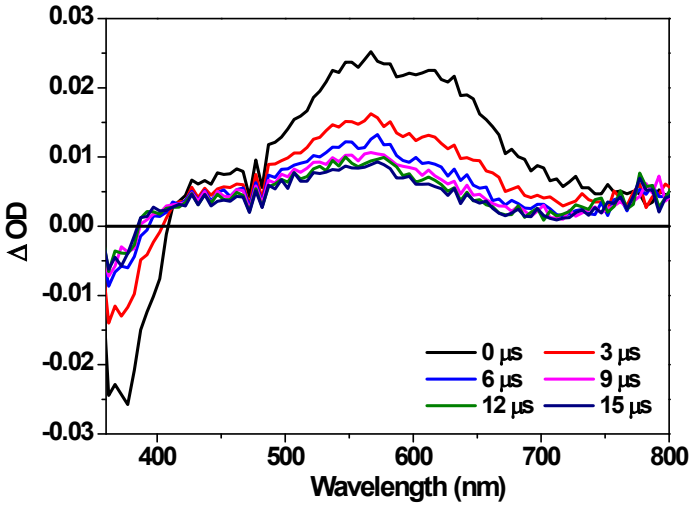

Figure S18. Time-resolved transient difference absorption spectra of **2** in toluene (λ_{ex} = 355 nm, A_{355} = 0.4 in a 1-cm cuvette).

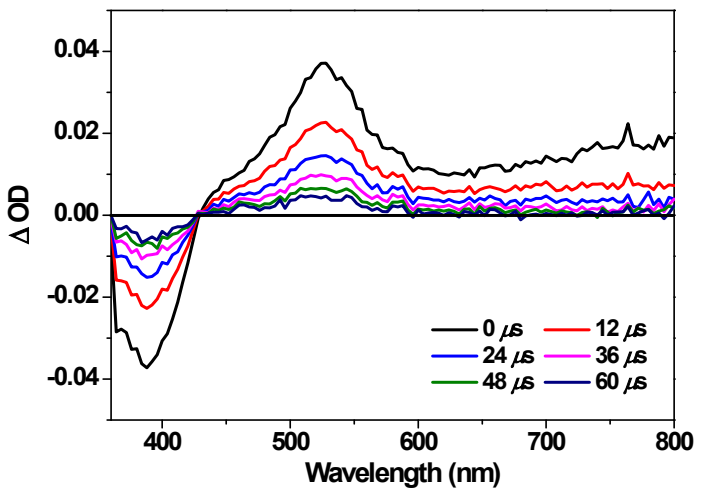

Figure S19. Time-resolved transient difference absorption spectra of **3** in toluene (λ_{ex} = 355 nm, A_{355} = 0.4 in a 1-cm cuvette).

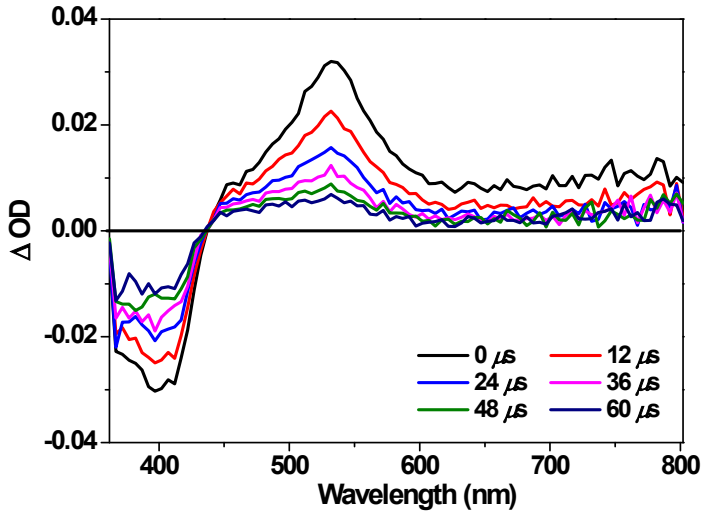

Figure S20. Time-resolved transient difference absorption spectra of **4** in toluene (λ_{ex} = 355 nm, A_{355} = 0.4 in a 1-cm cuvette).

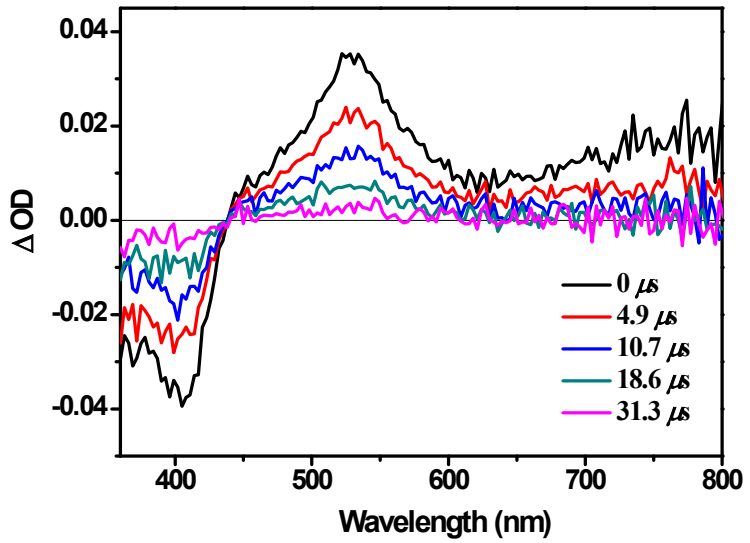

Figure S21. Time-resolved transient difference absorption spectra of **5** in toluene (λ_{ex} = 355 nm, A_{355} = 0.4 in a 1-cm cuvette).

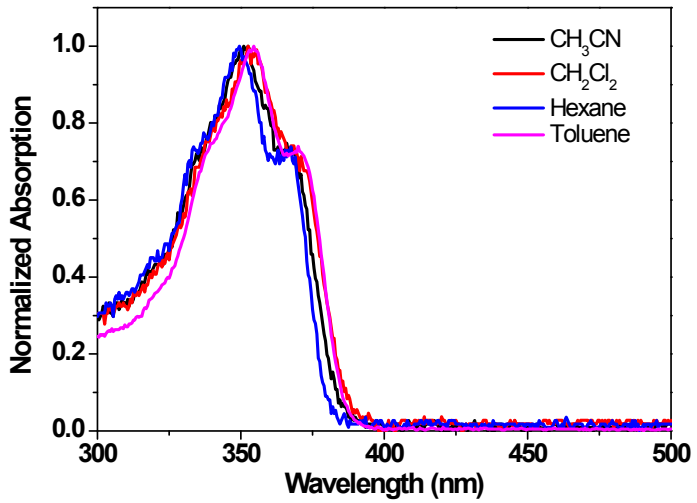

Figure S22. Normalized electronic absorption of **1-L** in different solvents.

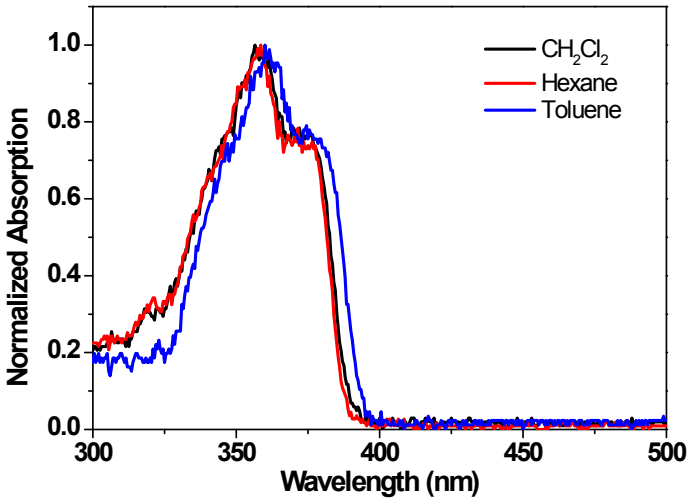

Figure S23. Normalized electronic absorption of **2-L** in different solvents.

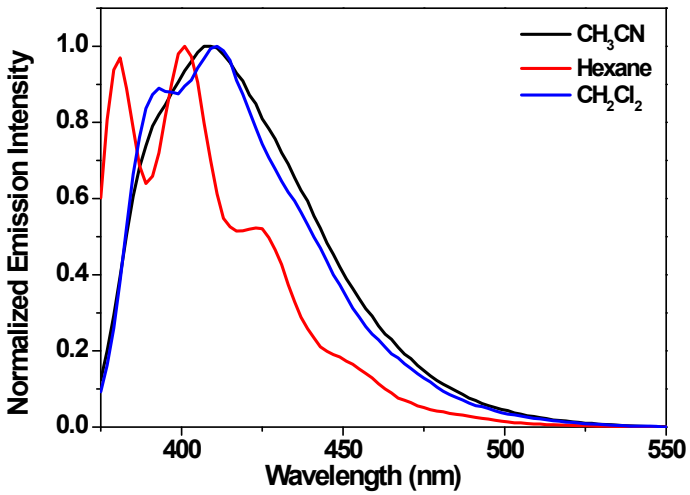

Figure S24. Normalized emission of **1-L** in different solvents (λ_{ex} = 365 nm).

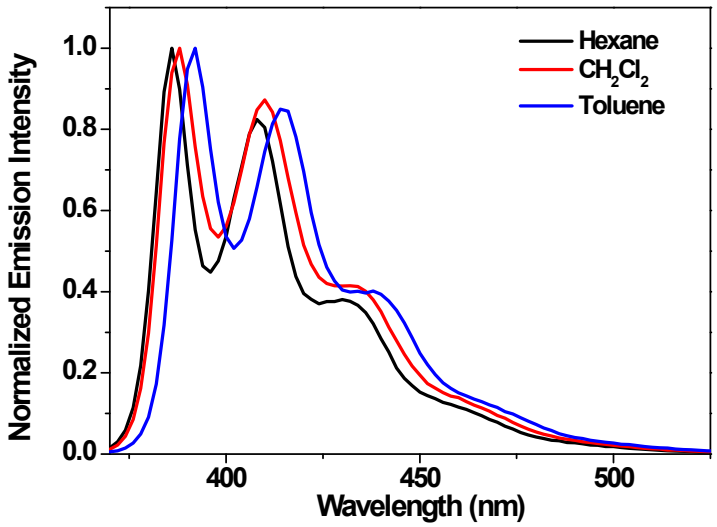

Figure S25. Normalized emission of **2-L** in different solvents (λ_{ex} = 365 nm).

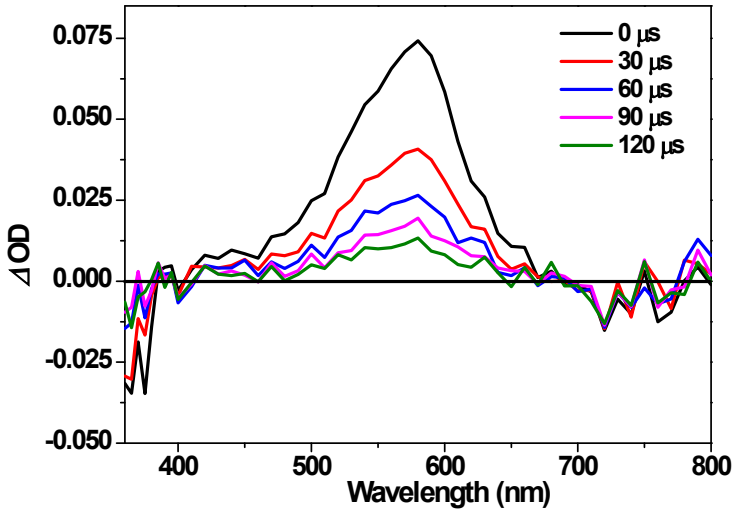

Figure S26. Time-resolved transient difference absorption spectra of **1-L** in toluene (λ_{ex} = 355 nm, A_{355} = 0.4 in a 1-cm cuvette).

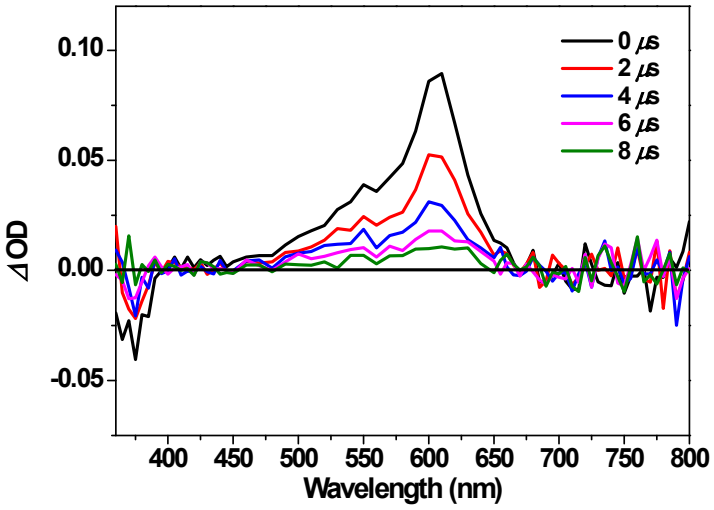

Figure S27. Time-resolved transient difference absorption spectra of **2-L** in toluene (λ_{ex} = 355 nm, A_{355} = 0.4 in a 1-cm cuvette).

Table S1. Emission quantum yields of **1-L** and **2-L** in different solvents.

	CH_2Cl_2	CH_3CN	Hexane	Toluene
1-L	0.58	0.58	0.49	-
2-L	0.71	-	0.68	0.67

Table S2. Emission characteristics of **3 - 5** in different solvents.

	λ / nm (τ / μs); Φ_{em}		
	Toluene	CH_2Cl_2	CH_3CN
3	518 (29.0 (83%), 1.15 (17%)), 556 (27.9 (89%), 1.17 (11%)), 604 (25.6 (85%), 1.53 (15%)); 0.22	519 (27.6 (77%), 1.26 (27%)), 557 (32.3 (89%), 1.43 (11%)), 598 (23.5 (81%), 1.51 (19%)), 653 (25.2 (76%), 1.36 (24%)); 0.44	519 (1.98), 557 (5.68), 595 (2.76), 648 (2.85); 0.16
4	520 (36.0 (92%), 1.25 (8%), 555 (34.1 (96%), 1.31 (4%), 595 (34.2 (78%), 2.40 (22%), 648 (24.3 (56%), 1.69 (44%)); 0.38	521 (23.66 (77%), 1.09 (23%)), 558 (31.41 (91%), 1.41 (8%)), 598 (22.16 (84%), 654 (10.29 (81%), 0.89 (19%); 0.35	521 (1.95), 558 (5.68), 598 (2.71), 647 (2.09); 0.21
5	519 (35.1), 555 (33.1), 594 (33.1 (85%), 2.87 (15%)), 648 (34.8 (68%), 2.61 (32%)); 0.45	519 (29.3), 556 (33.5), 595 (11.6), 650 (-); 0.33	518 (27.9), 558 (39.3), 595 (15.8), 650 (-); 0.31

Table S3. Natural Transition Orbitals (NTOs) contributing to the triplet emission of complex **1**. Optimization of the excited state have been started with several different initial guesses for the wavefunction choosing either the very lowest triplet state (root = 1) or the second lowest triplet state (root = 2) or the third lowest state (root = 3) initially taken at the ground state geometry of the triplet state.

Root	State (nm)	Hole	Electron
1	T_1 721	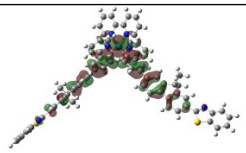	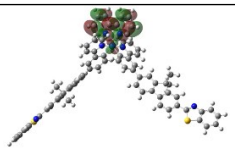
	T_2 586	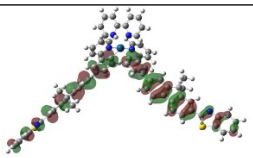	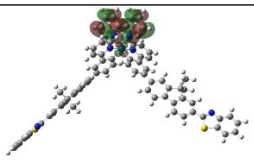
	T_3 544	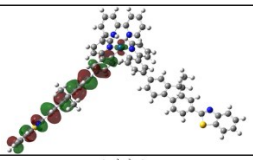	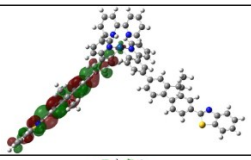
2	T_1 691	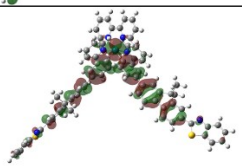	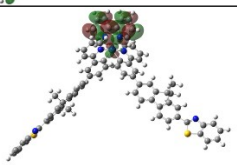
	T_2 612	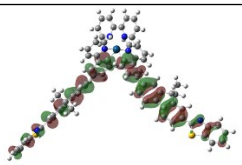	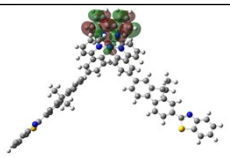
	T_3 559	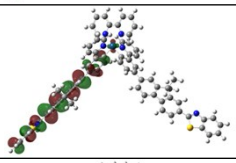	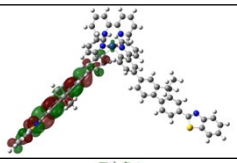
3	T_1 691	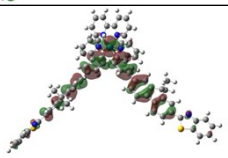	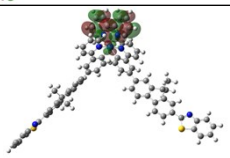
	T_2 559	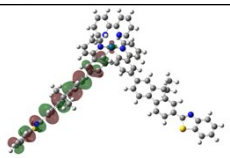	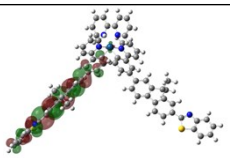
	T_3 612	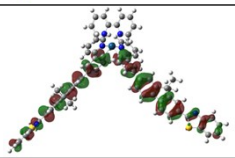	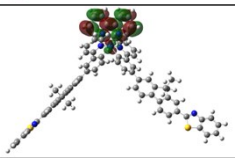

Table S4. NTOs contributing to the triplet emission calculated in a same way as in Table S3 but for complex **2**.

Root	State (nm)	Hole	Electron
1	T_1 751	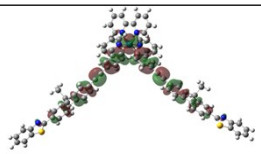	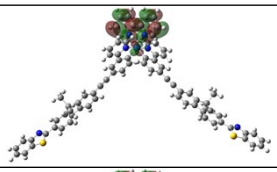
	T_2 632	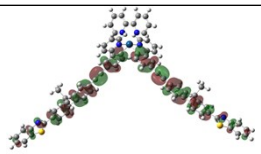	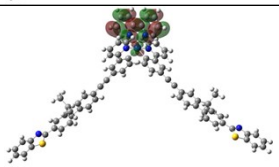
	T_3 595	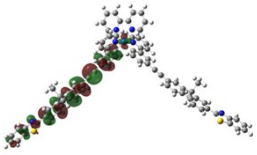	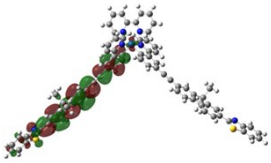
2	T_1 725	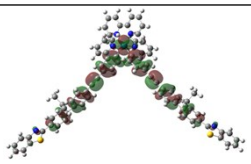	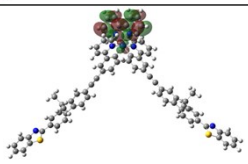
	T_2 654	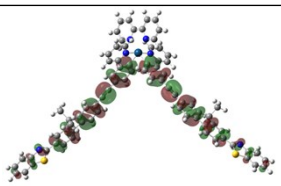	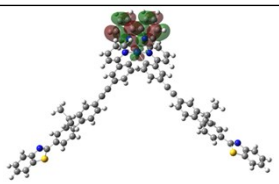
	T_3 604	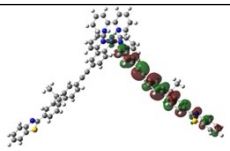	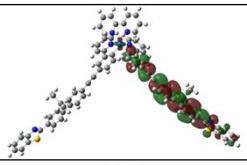
3	T_1 569	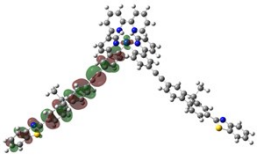	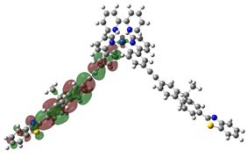
	T_2 621	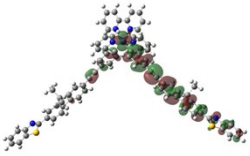	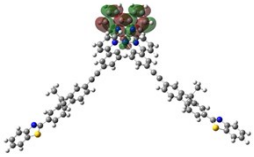
	T_3 771	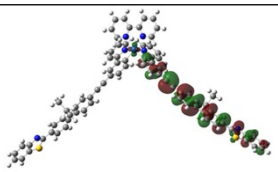	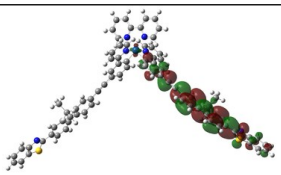

Table S5. NTOs contributing to the triplet emission calculated in a same way as in Table S3 but for complex **3**.

Root	State (nm)	Hole	Electron
1	T_1 738	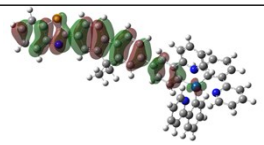	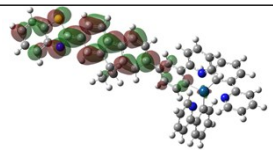
	T_2 495	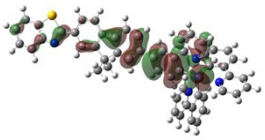	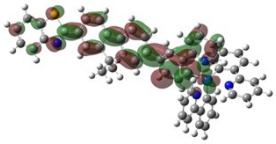
	T_3 458	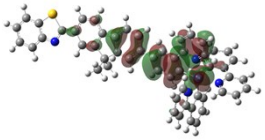	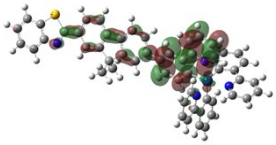
2	T_1 575	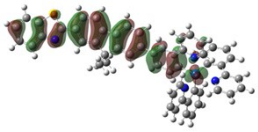	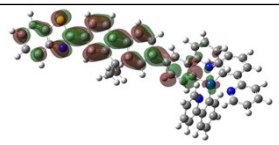
	T_2 545	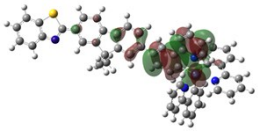	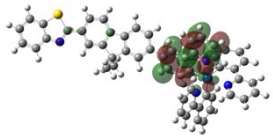
	T_3 454	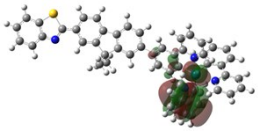	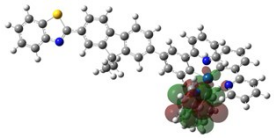

Table S6. NTOs contributing to the triplet emission calculated in a same way as in Table S3 but for complex **4**.

Root	State (nm)	Hole	Electron
1	T_1 738	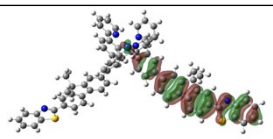	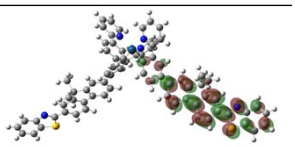
	T_2 533	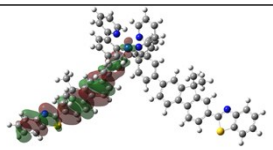	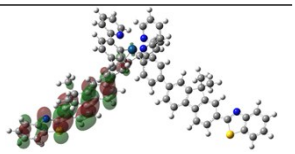
	T_3 494	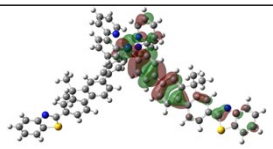	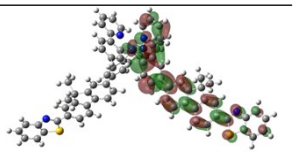
2	T_1 534	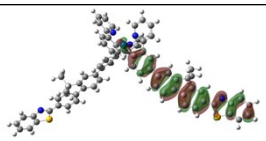	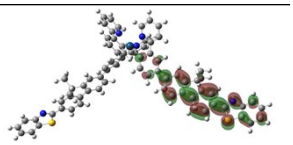
	T_2 738	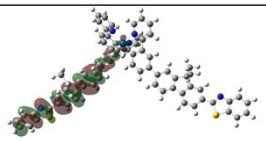	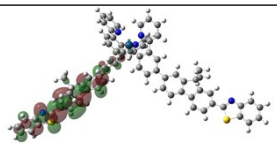
	T_3 493	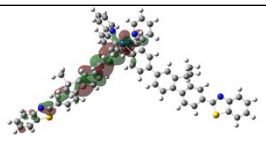	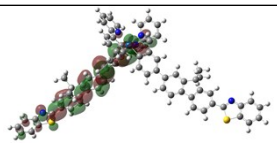

Table S7. NTOs contributing to the triplet emission calculated in a same way as in Table S3 but for complex **5**.

Root	State (nm)	Hole	Electron
1	T_1 738	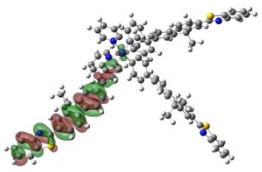	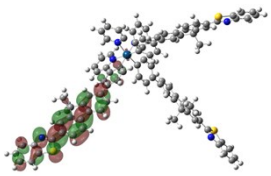
	T_2 533	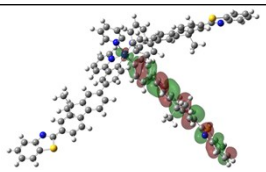	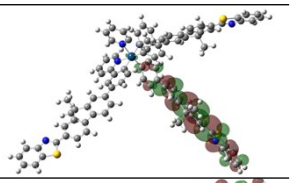
	T_3 533	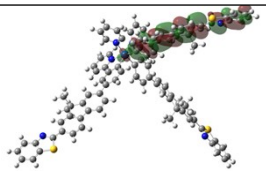	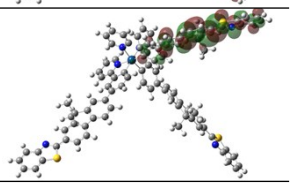
	T_4 492	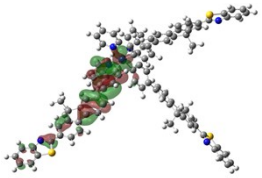	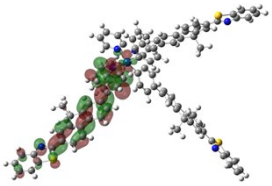
2	T_1 533	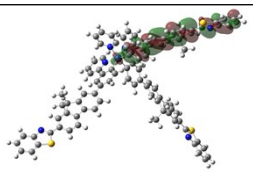	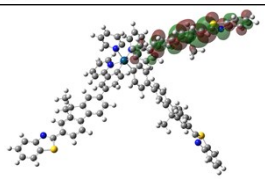
	T_2 738	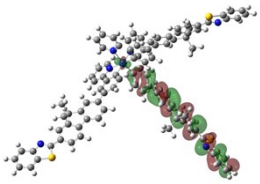	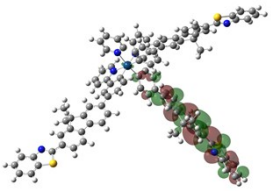
	T_3 532	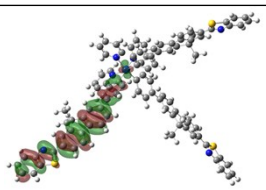	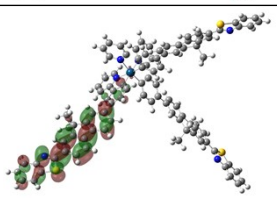

Table S8. TA lifetimes of the *fac*-isomers of **3 – 5** monitored at different wavelengths

	750 nm	700 nm	650 nm
3	34.5 μs	34.5 μs	33.3 μs
4	37.3 μs	35.0 μs	39.0 μs
5	36.1 μs	39.9 μs	38.6 μs